Journal of Applied Polymer Science

TAT-Modified Mixed Micelles as Biodegradable Targeting and Delivering System for Cancer Therapeutics

Xiaoyuan Li,[1] Mingzhe Wang,[1] Changbai Liu,[2] Xiabin Jing,[1] Yubin Huang[1]

[1]State Key Laboratory of Polymer Physics and Chemistry, Changchun Institute of Applied Chemistry, Chinese Academy of Sciences, Changchun 130022, China

[2]The Institute of Molecular Biology, Three Gorges University, Yichang 443002, China

Correspondence to: Y. Huang (E-mail: ybhuang@ciac.jl.cn) or C. Liu (E-mail: changbail@yahoo.com).

ABSTRACT: A mixed micellar system of novel function was designed and synthesized by co-assembling TAT (cell penetrating peptide)-modified poly (ethylene glycol)-poly(L-lactide) (PEG-PLA) copolymer with the drug-conjugated poly(ethylene glycol)-*b*-poly(L-lactide-*co*-2-methyl-2-carboxyl-propylene carbonate) (mPEG-*b*-P(LA-*co*-MCC)) copolymer. UV-Vis, Matrix-assisted laser desorption/ionization time-of-flight, and XPS were used to ensure the successful modification of the copolymers with TAT and anti-tumor drugs. The size of spherical nanomicelles increased from 50 to 60 nm as of empty polymeric micelles to 100–150 nm as of drug-loaded ones, determined by dynamic light scattering and TEM. Daunorubicin was selected as model drug for *in vitro* evaluations on different cell lines. 3-(4,5-Dimethylthiazol-2-yl)-2,5-diphenyltetrazolium bromide assay clearly indicated an improved cell growth inhibition of the TAT-modified mixed micelles. While green fluorescent protein was used as a marker for the mixed micelle, small amount of DMSO was necessary to enhance the accumulation of the mixed micelles in cell lines Caski. Mediated by TAT, mixed micelles containing Apoptin (a tumor-specific apoptosis drug) showed higher level of tumor cell internalization and growth inhibition than that of mixed micelles without TAT modification. © 2013 Wiley Periodicals, Inc. J. Appl. Polym. Sci. 130: 4598–4607, 2013

KEYWORDS: biodegradable; drug delivery systems; micelles

Received 27 February 2013; accepted 5 July 2013; Published online 29 July 2013
DOI: 10.1002/app.39744

INTRODUCTION

Chemotherapy is one of the essential treatments for tumors. However, high hydrophobicity of most chemotherapeutic drugs restricts their clinical use because of their severe side effects, such as hypersensitivity, nephrotoxicity, and neurotoxicity, resulting from the assistant organic solvents.[1–3] Therefore, nanomicelles or capsules based on synthetic polymers have been extensively studied as drug delivery vehicles for entrapment of those water insoluble drugs.[4] These vehicle systems have advantages of controlled drug release, subcellular size, and biocompatibility.

PEGylation is one of the most popular method and effective strategies providing not only water solubility to the vehicle system, but also immuno-shielding from reticular endothelium system, thus prolong the circulation time. With the PEG-based shell, the nanomicelles or capsules could also avoid the adsorption of proteins and adhesion of cells in biological media. With the approval of FDA, poly(ethylene glycol)-poly(L-lactide) (PEG-PLA) has been widely used in the encapsulation of hydrophobic anticancer drug such as paclitaxel to improve water solubility and biocompatibility as well as anti-tumor efficacy thanks to enhanced permeability and retention (EPR) effect.[5] However, the encapsulation efficacy was not always satisfying, and the leakage of loaded drugs from micelles which caused initial burst often happened.

Instead, specific chemical conjugation between polymer and drug through degradable bond is more preferable as it would not disrupt the drug efficacy. The conjugation would not only enable the extended encapsulation of hydrophilic drugs into micelles, but also restrict the drug molecules from escaping from the endothelial phagocytose. However, limited active groups of the hydrophobic compartment PLA constrain the multifunctional modification and characterization. Copolymerization of lactide with monomers bearing active groups, like 2-methyl-2-carboxyl-propylenecarbonate (MCC) with carboxyl group, would circumvent this deficiency.[6] The amphiphilic nature of poly (ethylene glycol)-block-poly (L-lactide-*co*-2-methyl-2-carboxyl-propylenecarbonate) [mPEG-*b*-P(LA-*co*-MCC)] and its derivatives also ensures that they can self-assemble into micelles or spherical colloidal nanomicelles.[7]

Recently, cell penetrating peptides (CPPs) have been used as a promising tool to transduce presynthesized therapeutic molecules which possess low membrane permeability, to circumvent

the chemotherapeutic resistance in cells and to increase the cytotoxicity against cancers.[8,9] A typical example of CPPs is TAT, a basic peptide segment corresponding to the positions 48–60 of Tat protein which is a transcription regulator protein of HIV-1. Cytoplasmic uptake mediated by TAT ranges from drug conjugated polymers, bacteriophages, magnetic nanoparticles of about 10–20 nm in diameter to even liposomes having a diameter of nearly 200 nm.[10–13]

Although tumor accumulation of the drug-loading system is improved by the EPR effect and TAT mediation, the side effects on normal cells still cannot be completely eliminated. Apoptin, which is the encoded protein of a chicken anemia virus VP3 gene, has been found to be a tumor specific localization drug to induce apoptosis of human tumor cells through nucleic localization without damaging the normal cells.[14,15] Combination of Apoptin with amphiphilic copolymers would enable the self-assembled system with superior functions of sustained release and specific apoptosis of the tumor cells.

In our research, to avoid complicated protection and deprotection procedures on a single copolymer chain, we adopted the co-assembling strategy to make mixed micelles composed of TAT-PEG-PLA and drug-loaded mPEG-*b*-P(LA-*co*-MCC) copolymer. Both copolymers had the similar amphiphilic composition and comparable chain length. Previous work has confirmed the enhanced cytotoxicity of TAT-modified micelles loaded with anticancer drugs, such as the paclitaxel loaded polyethyleneglycol-phosphatidylethanolamine (PEG-PE) micelles with distal modification of TAT and the polymeric micelles constitute of two block copolymers of poly(L-lactic acid)-*b*-poly(ethylene glycol)-*b*-poly(L-histidine)-TAT (PLA-*b*-PEG-*b*-polyHis-TAT) and poly(L-histidine)-*b*-poly(ethylene glycol) (polyHis-*b*-PEG).[16,17] Based on these work, we aimed at developing a more reliable drug delivery system with enhanced membrane penetration and nucleic localization apoptosis. TAT and Apoptin were, respectively, conjugated to the surface and core of the mixed micelles, which were endowed with the possibility to precisely control of drug content through the degradable amide linkage on MCC part. To avoid unnecessary waste of the expensive Apoptin, a hydrophobic fluorescent drug (Daunorubicin, DNR) and a hydrophilic green fluorescent protein (GFP) were both used as models of Apoptin to visualize and simulate the TAT-mediated penetration and accumulation of the mixed micelles into the tumor site.

MATERIALS AND METHODS

Materials

Monomethoxy-poly (ethylene glycol) (mPEG) with molecular weight of 2 kDa and 5 kDa, were purchased from Sigma. Prior to use, mPEG was dried by an azeotropic distillation in toluene. L-Lactide (LA) was prepared in our own laboratory and recrystallized from ethyl acetate three times before use. 2-methyl-2-benzoxycarbonyl-propylene carbonate (MBC) was prepared according to the literature.[18] Diethyl zinc ($ZnEt_2$) was kindly supplied by Prof. Wang Xianhong's group in CIAC. Palladium hydroxide on activated charcoal ($Pd(OH)_2$/C, 20%) was obtained from Shanxi Kaida Chemical Industry Corporation. DNR in the form of hydrochloride salt was purchased from Zhejiang Hisun Pharmaceutical. Lysine-modified CPP TAT, GFP, Apoptin, and peptide NCON (KALGISYGGKKGGSKALGISYGGKKSGGGSKK, a control peptide without any function) were purchased from Beijing SBS Genetech. Toluene was dried and distilled in the presence of sodium. Dichloromethane was treated with hexamethylene diisocyanate for 5 h at 50°C and distilled to remove any traces of amine and alcohol. *N,N*-Dimethylformamide (DMF) was dried over CaH_2 and then distilled under reduced pressure before use. Trypsin and RPMI 1640 medium were purchased from GibcoBRL. Fetal bovine serum (FBS) was purchased from Cellmans Biologic, China. 3-(4,5-Dimethylthiazol-2-yl)-2,5-diphenyltetrazolium bromide (MTT) was purchased from Sigma. All other reagents were commercially available and used as received. All the polymers that were employed for cell culture studies were further purified by dialyzing extensively against distilled water (SpectraPor MWCO = 3.5 kDa) and lyophilized.

Synthesis of TAT-Modified PEG-PLA (TAT-PEG-PLA)

Amphiphilic block copolymer α-Carboxyl-ω-hydroxyl PEG-PLA was first synthesized according to our previous work.[19] Briefly, PEG (5 kDa) bearing an allyl group at one end and a hydroxyl group at the other was first obtained through allyoxyl anion ROP of ethylene oxide. Then the hydroxyl end of this PEG was used to initiate the ROP of LA with $Sn(Oct)_2$ as catalyst to obtain allyl-PEG–PLA (MW of PLA segment was 2 kDa). Radical thiol-ene reactions between allyl-PEG-PLA and 3-mercaptopropionic acid were carried out in THF under UV light at room temperature to replace allyl group with carboxyl one.

Because of the limited amount of TAT and the potential disturbance from the hydroxyl group on the end of the PLA chain, the above obtained PEG-PLA was first self-assembled into micelles by dissolving the copolymer in THF with titration of water (double volume of THF) at slow speed through peristaltic pump. (Scheme 1) After THF removal and freeze-drying, the micelle powder was prepared. The micelle powder was redispersed in water and reacted with Sulfo-NHS and EDC•HCl (copolymer/Sulfo-NHS/EDC•HCl, 1/8/8, mol/mol/mol) at 0°C for 1.5 h. Purified with water washing and centrifugation, TAT (10 mg) was added. The reaction was kept under a circumstance of 0°C for 2 h, followed by 12 h stirring at room temperature. After dialysis (MW cut-off 3.5 kDa) against water for 3 days to get rid of the free TAT, the TAT-modified PEG-PLA 3 was obtained. The peptide NCON was also conjugated with the PEG-PLA copolymer in the same way to act as a control.

Synthesis of Drug-Loaded mPEG-b-P(LA-co-MCC)

According to our previous work,[6] amphiphilic block copolymer mPEG-*b*-P(LA-*co*-MBC) was prepared in bulk by ring-opening polymerization of LA and MBC in the presence of mPEG as a macro-initiator and diethyl zinc as a catalyst. A series of these copolymers with different molecular weight and composition were synthesized (Table I), and the characterization data of P5 is shown below as an example. P5: 1H NMR (DMSO, δ ppm vs. tetramethylsilane): 5.21 (m, 1H, —C(O)—CH(CH3)—O—), 4.20 (s, 0.26H, —O—CH2—C(CH3)(COOH)—), 3.51 (s, 16H, —CH2—CH2—O—), 1.47 (d, 3H, —O—CH(CH3)—C(O)—).

Applied Polymer SCIENCE

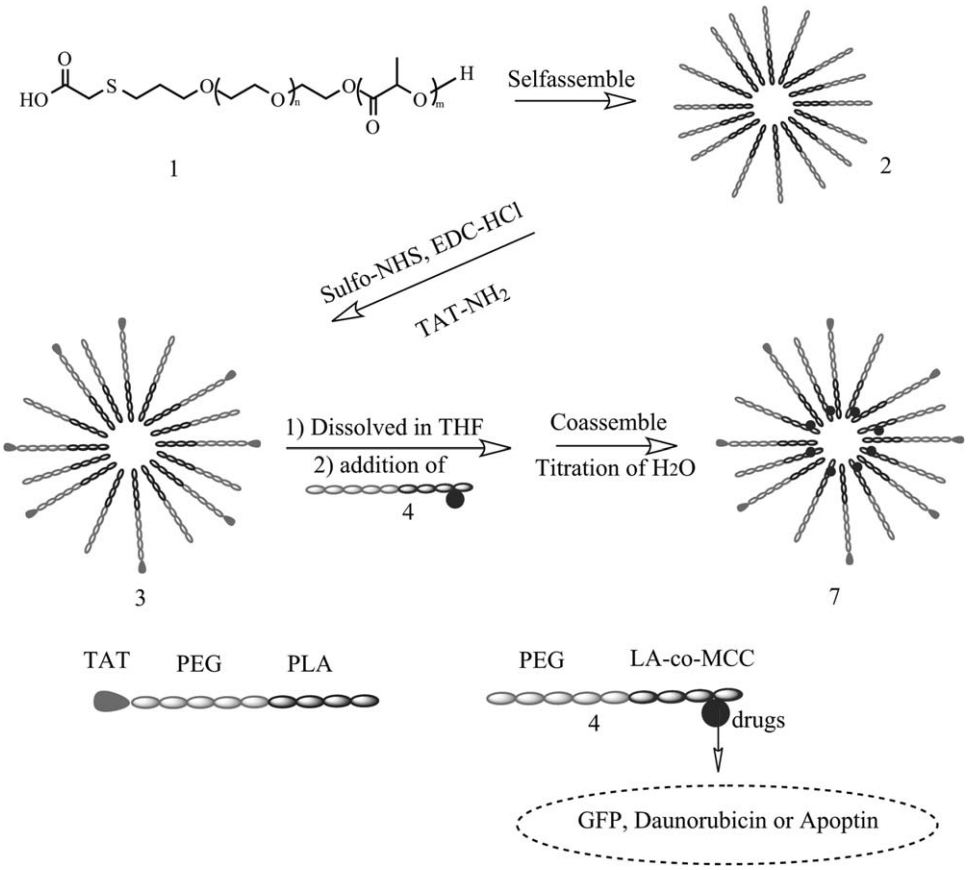

Scheme 1. Preparation of multifunctional mixed micelles.

The subsequent catalytic hydrogenation of mPEG-*b*-P(LA-*co*-MBC) with palladium hydroxide on activated charcoal (20%) was carried out to obtain the corresponding linear copolymer mPEG-*b*-P(LA-*co*-MCC) with pendant carboxyl groups. The activation of pendent carboxyl group was conducted under nitrogen to further react with drug molecules (Scheme 2). As an example, in a dried flask, 0.12 g of P5 was dissolved in 10 mL of anhydrous DMF. 8.35 mg of NHS, 22 mg of DCC, and 1.44 mg of DMAP were added into the above solution at 0°C. The solution was kept being stirred for 2 h at 0°C and 22 h at room temperature. After separation of the by-product dicyclohexylurea, the filtrate was condensed and poured into an excess amount of diethyl ether. After centrifugation, the carboxyl-activated product 7 was dried in vacuum (yield: 83%). An excess amount of 7 (0.048 g) was then reacted with GFP (0.026 g) in anhydrous DMF (5 mL) with TEA (10 μL) as catalyst. The mixture was kept being stirred at 0°C overnight in dark. The solvent was then dialyzed against DMF with a cellulose membrane (MW cut-off 3.5 kDa) for 1 day, followed by dialysis against distilled water for 3 days. The final product 4 was

Table I. Characteristic of Copolymer mPEG-*b*-P(LA-*co*-MBC)

Copolymer no.	Mn of mPEG (g/mol)	Mn of PLA (g/mol)[a]	Mn of MBC (g/mol)[a]	Mn of copolymer (g/mol)[b]	PDI[c]	CMC (mg/L)	Size of micelles (nm)[c]
P 1	2000	867	320	5827	1.14	1.31	90–130
P 2	2000	847	639	5170	1.20	2.45	130–165
P 3	2000	1515	502	6806	1.19	0.84	200–250
P 4	5000	1751	1277	11520	1.06	1.68	40–80
P 5	5000	2601	846	17336	1.14	2.06	60–90
P 6	5000	4648	1285	14700	1.18	1.05	35–75

[a] Determined by ^{1}H NMR in $CDCl_3$ solution.
[b] Determined by GPC in $CHCl_3$.
[c] Determined by DLS in $CHCl_3$.

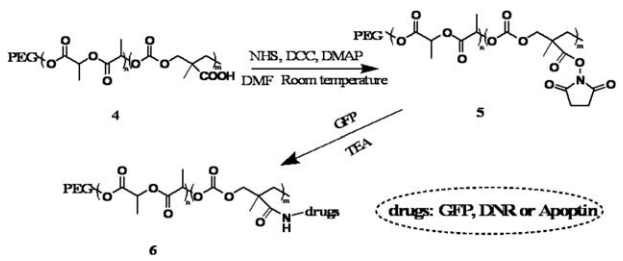

Scheme 2. Conjugation process of drugs with mPEG-*b*-P(LA-*co*-MCC).

obtained after subsequent freeze-drying (yield: 66%). Besides GFP, DNR, and Apoptin were also conjugated to mPEG-*b*-P(LA-*co*-MCC) using the same method described above.

Formation of the Mixed Micelles

The powder of TAT-PEG-PLA micelles 3 were first dissolved in THF to get micelles dissociated and then 4 was added to the solution in the ratio of 4 : 1. The final volume of THF was about 5 mL and 10 mL of doubly distilled water was added with agitation. After being removed of THF on the rotating evaporator device, the mixed micelles 5 were prepared (Scheme 1).

Characterization

The 1H NMR spectra were recorded on a Bruker AV300M spectrometer in CDCl3 or DMSO-*d*6 at 25°C. Chemical shifts were given in parts per million from that of TMS as an internal reference. Gel permeation chromatography (GPC) measurements were conducted with a Waters 410 GPC with CHCl3 for block copolymers or THF for allyl-PEG as eluent (flow rate: 1 mL/min, at 35°C). The molecular weights were calibrated with polystyrene standards (molecular weight range: 0.5–30 kDa). Critical micellar concentration (CMC) was determined using pyrene as a fluorescence probe and the steady state fluorescence spectra were obtained by a Perkin-Elmer LS50B luminescence spectrometer. Particle size and size distribution of the micelles were determined by dynamic light scattering (DLS) with a vertically polarized He-Ne laser (DAWN EOS, Wyatt Technology). The scattering angle was fixed at 90°, and the measurement was carried out at room temperature. The sample solutions were filtered using disposable 0.45 μm Millipore filters before analysis. The morphology of the micelles was measured by TEM performed on a JEOL JEM-1011 electron microscope operating at an acceleration voltage of 100 kV. To prepare specimens for TEM, a drop of micelle solution (0.01 mg/mL) was deposited onto a copper grid. The specimens were air-dried and measured at room temperature. The surface electrical charge analyses were completed using a zeta potential analyzer from Brookhaven by electrophoretic light scattering method. The measurements were performed in triplicate at a temperature of 25°C with field strength of 10 V cm^{-1}. Matrix-assisted laser desorption/ionization time-of-flight mass (MALDI-TOF MS) spectra were recorded using Bruker Autoflex III TOF/TOF. Sinapinic acid (SA) was used as the matrix for the ionization. Two solutions were prepared before detection: the sample solution (10 mg/mL in 0.1% TFA aqueous solution) and the matrix solution (saturated SA dissolved in acetonitrile/water solution, acetonitrile/water = 1 : 2, v/v). Two solutions were mixed together (volume ratio 1 : 1) and 2 μL of the mixture was introduced to the probe (laser repetition rate, 200 Hz; ion source voltage, 120 kV; linear detector voltage, 1.572 kV).

In Vitro Evaluation

Hela cells were used to evaluate the biocompatibility and cytotoxicity of the copolymers. Different cell lines: Hela, Caski, A549 and L929 were employed to comprehensively evaluate the anticancer efficiency of our micelle system. The cells were grown in RPMI 1640 supplemented with 10% FBS, 100 U/mL penicillin, and 100 mg/L streptomycin. Before the experiments, the cells were grown to 70–80% confluency in an incubator at 37°C, supplied with 5% CO_2. Cell viability was examined after incubation with the copolymer at various concentrations for 24 h and the status of the cells was observed using inverted fluorescence microscope (TE2000-U, Nikon). Three pictures of the cells for each sample were taken with a DXM1200F digital camera (Nikon). For the evaluation of anticancer efficiency of mixed micelles, the cells were treated with different types of mixed micelles at various concentrations for 24 h and the results were quantified by MTT assay. In brief, 5×10^3 cells per well were seeded into 96-well plates. After 24 h incubation, the cells were treated with different concentrations of mixed micelles or pure drug molecules and kept exposure for another 24 h. Subsequently, 20 μL MTT (5 mg/mL) was added to each well and reacted for 4 h in an incubator at 37°C. After pouring out the liquid, 150 μL of DMSO was added to each well to dissolve the purple formazan crystals. The plates were left to mix thoroughly on a plate shaker for 5 min and the absorbance at 490 nm was measured using a microplate reader. The results from the readings were expressed as a percentage of the control. The DMSO enhancement effect for TAT penetrating was carried out according to our previous work.[8] To determine the cellular uptake efficiency, Hela cells (2×10^5) were seeded on slides in a six-well plate for 24 h. The cells were incubated for 0.5 h with TAT-modified mixed micelle that contained DNR (0.01 mg/mL). Then the cells were washed twice with cold PBS and fixed with 4% formaldehyde. After stained with DAPI for the nucleus, the slides were mounted and observed with an Olympus FV1000 confocal laser scanning microscope (CLSM) imaging system (Japan).

RESULTS AND DISCUSSION

Synthesis of TAT-Modified PEG-PLA

Self-assembled polymeric micelles, TAT-mediated cell membrane penetration and active-targeting induced tumor cell apoptosis are the main concerns of our research. Amphiphilic copolymers are well known of forming the self-assembled micelles. In this work, PEG-PLA is chosen as the basic structure of the amphiphilic copolymer. It is not only because of the biodegradable and biocompatible nature of the copolymer, but also due to the FDA approval for PEG and PLA in clinical use.

In order to realize the enhanced penetration through cell membrane, TAT should be located on the surface of the micelle. Therefore, a new copolymer, HOOC-PEG_{5000}-PLA_{2000}-OH, was prepared through radical-mediated thiol-ene reaction. The terminal carboxyl group on the end of PEG segment could be used to react with amino group of lysine residue on the end of

Applied Polymer SCIENCE

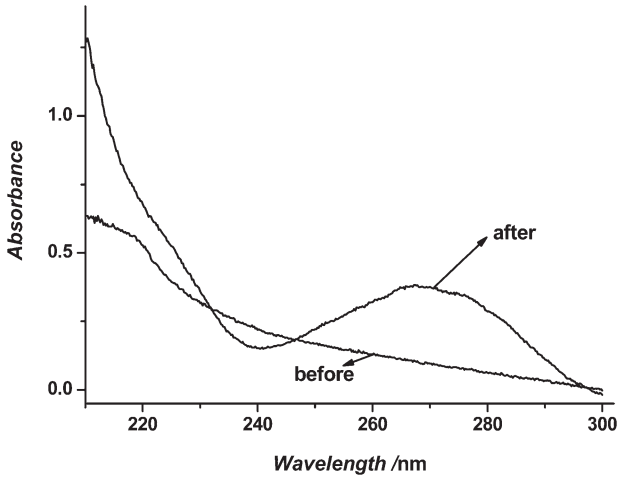

Figure 1. UV-Vis spectra of TAT-modified PEG-PLA micelles.

TAT sequence, however, the hydroxyl group on the end of PLA segment would probably interfere with the conjugation of TAT to PEG. For this reason, PEG-PLA with functional groups was first self-assembled to micelles. By this treatment, the carboxyl groups on PEG end would be exposed to the outer phase of the micelles. At the same time, the hydroxyl groups on PLA end could be encapsulated into the micelle core without contact with TAT. Finally, TAT with lysine residue was stabilized on the hydrophilic surface of the PEG-PLA micelles via amidation reaction. From Figure 1, new adsorption peak around 270 nm corresponding to TAT was observed in the UV-Vis spectra. The XPS results also clearly showed the existence of N element, indicating the presence of TAT on the surface of the PEG-PLA micelles (Figure 2).

Synthesis of Drug-Loaded mPEG-b-P(LA-*co*-MCC)

Unlike TAT modification, the drug molecules should be bound to the hydrophobic segment and encapsulated into the micelle core to obtain the sustained release capacity. A simple consideration for drug-loading is to conjugate the drug to the PLA end of the TAT-PEG-PLA copolymer (like TAT-PEG-PLA-Drug). In fact, this kind of designation has many latent difficulties. For example, the active groups on TAT would definitely disturb the reaction between drug and PLA end, and bring many uncertain impurities to the product. Instead, the mixed micelles system, which is formed by mixing together the different kinds of copolymers that have the similar amphiphilic composition and comparable chain length, would be a more convenient choice to introduce both TAT and drugs in one carrying system.

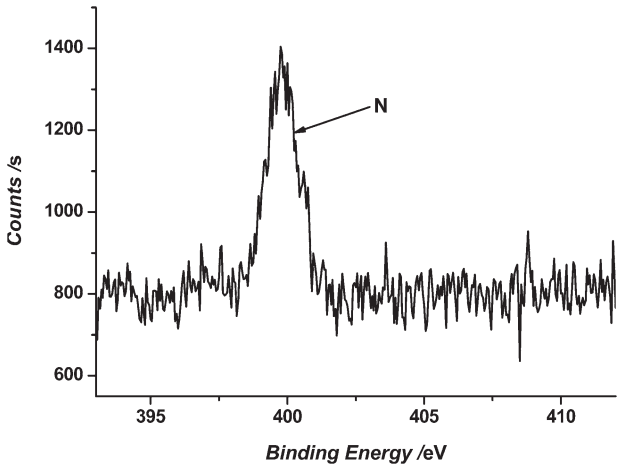

Figure 2. XPS spectra of TAT-modified PEG-PLA micelles.

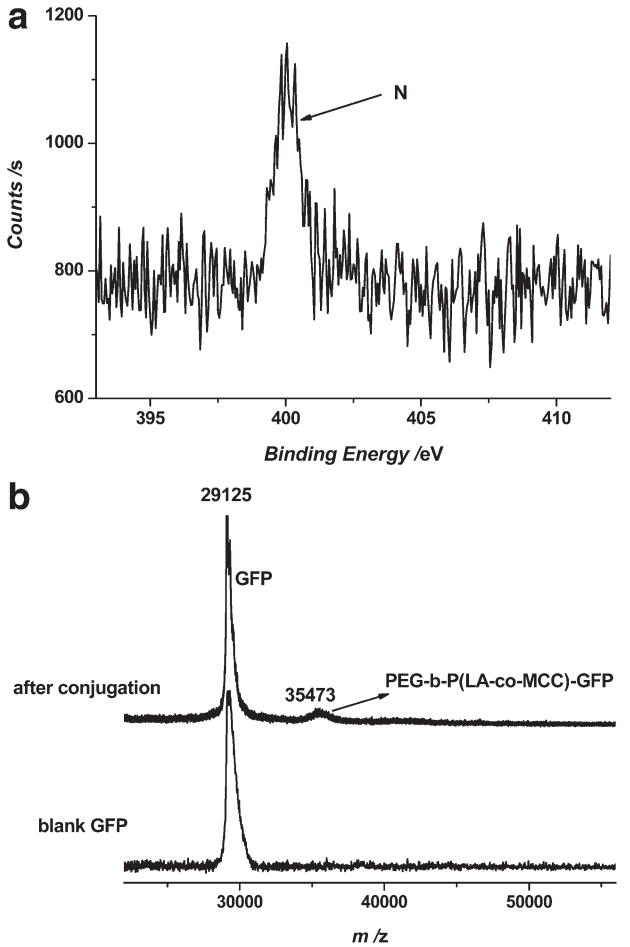

Figure 3. XPS (a) and MALDI-TOF (b) spectra of PEG-P(LA-MCC)-GFP.

In order to incorporate much more amount of drugs in the micelle system, MBC with protected carboxyl group was copolymerized with LA using PEG as macro-initiator. Table I showed that controllable carboxyl contents were obtained with different feeding ratio of the monomers. Because of the amphiphilic nature, mPEG-*b*-P(LA-*co*-MBC) could also self-assemble into nanoscale micelles. Generally, the sizes of mPEG-P(LA-*co*-MBC) micelles decreased with longer PEG chain, and increased with hydrophobic segment, which is similar to the report.[20] TEM results (data not shown) showed that all the copolymer micelles had the spherical morphology. Since spherical nanocarriers with diameters from 40 to 300 nm are all available for passive targeting,[21] P5 micelles, with the narrowest distribution, were selected as the carriers for later drug loading. After deprotection procedure, the carboxyl groups could be exposed for further conjugation with drugs. 1H-NMR spectrum revealed that the signals belonging to protective groups at 7.3 ppm disappeared; while the other proton signals did not change indicating that polymer

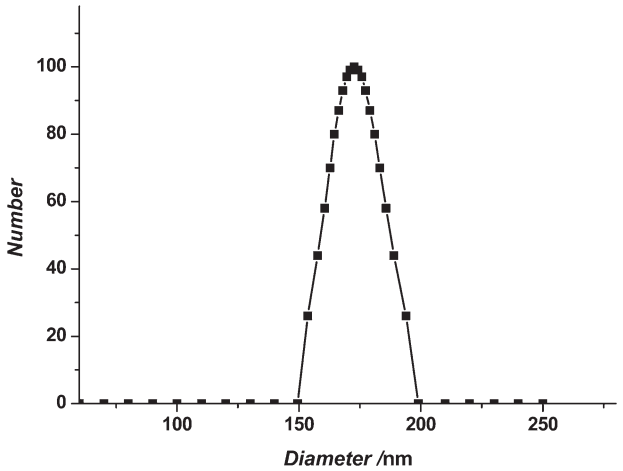

Figure 4. DLS of mixed micelles composed of PEG_{2000}-PLA_{2000} and P3.

structure was kept intact (data not shown). Conjugation of GFP to the side carboxyl groups of mPEG-*b*-P(LA-*co*-MCC) was confirmed by XPS since there was no N element in the copolymer before reaction [Figure 3(a)]. MALDI-TOF MS also revealed that the successful conjugation of GFP to mPEG-*b*-P(LA-*co*-MCC) [Figure 3(b)]. For DNR conjugation, the purified products presented strong fluorescence observed by the inverted fluorescence microscope (figures not shown). DNR content was further determined to be 10 wt % in the polymeric conjugate by measuring the UV absorbance of a DMSO solution of the conjugates at 480 nm.

Preparation and Characterization of the Multifunctional Mixed Micelles

Comprehensive therapy containing anti-cancer drugs, which integrate advantages such as long blood circulation time, high drug efficacy, and targeting impact is always preferable. However, from time to time, it is more difficult and expensive to achieve this goal by using one kind of copolymer. Nevertheless, the mixed micelle strategy has been applied and proven to be an effective choice by our group.[22] In order to confirm the validity of this method for our polymer systems, DLS was conducted according to the literature.[23] As shown in Figure 4, there is only one single peak for the polymer mixed micelles. The original sizes of PEG-PLA micelles and PEG-P(LA-*co*-MCC) micelles were 70 nm and 200 nm, respectively. The absence of these peaks indicated the successful preparation of mixed micelles. In this study, mixed micelles composed of comparable

Table II. Compositions of a Series of Multifunctional Mixed Micelles

Mixed micelle no.	Constitute 1	Constitute 2
MM1	TAT-PEG-PLA	PEG-*b*-P(LA-*co*-MCC/DNR)
MM2	PEG-PLA	
MM3	TAT-PEG-PLA	PEG-*b*-P(LA-*co*-MCC/GFP)
MM4	NCON-PEG-PLA	
MM5	TAT-PEG-PLA	PEG-*b*-P(LA-*co*-MCC/ Apoptin)
MM6	NCON-PEG-PLA	

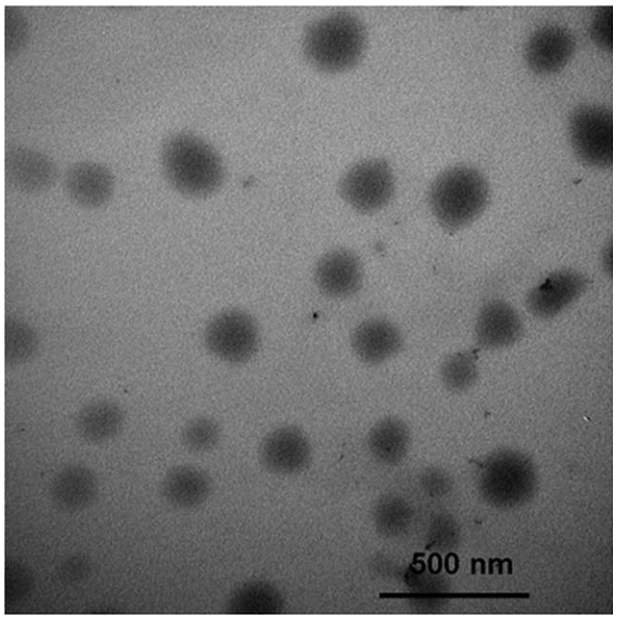

Figure 5. TEM image of MM3.

copolymer composition of Constitute 1 and 2 (Table II) were adopted to carry penetrating peptide TAT and drug molecules in the same drug-loading system. The molar ratio of the two constitutes was conservatively set to be 1 : 4 according to the research results from Xiong et al.,[24] who have developed RGD/TAT-functionalized virus-like micelles for siRNA delivery at peptide : polymer ratio of 1 : 5. Characteristic similarities between the two constitutes, which originated from the identical PEG length and comparable hydrophobic blocks' length, made it possible to form stable mixed micelles. The morphology and size were also confirmed by TEM (Figure 5) and DLS, showing larger spherical size in comparison with the copolymer micelles. Due to the limited amount of GFP and Apoptin, before the encapsulation of GFP and Apoptin, BSA was employed as a model protein to confirm the validity of the protein encapsulation. The UV-Vis spectra confirmed that after micelle formation at the isoelectric point of 4.6 for BSA, no protein absorbance was observed anymore. When we destroyed the micelles, the

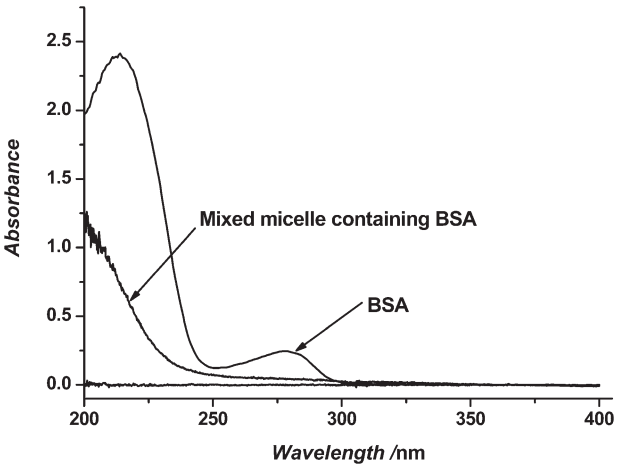

Figure 6. UV spectra of BSA and mixed micelles containing BSA.

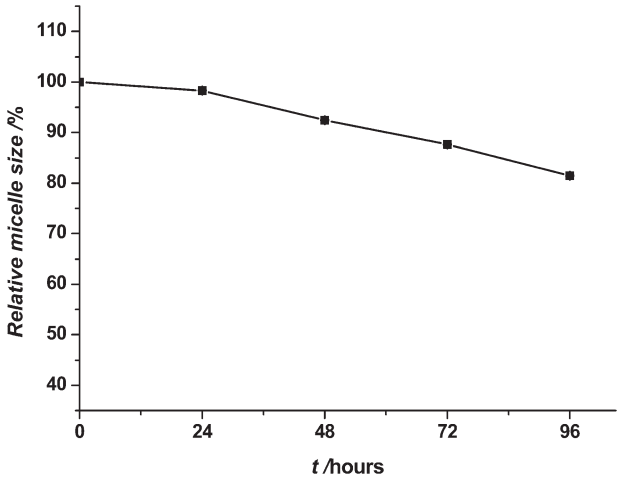

Figure 7. Mixed micelles stability. Size percentage of MM1 in RPMI 1640 with 10% FBS changed as a function of time.

absorbance of BSA again appeared. These indicated that protein molecules can be well entrapped within the micellar core (Figure 6). Furthermore, diameter of GFP containing group MM3 (120–160 nm) was larger than DNR containing group MM1 (80–110 nm) and Apoptin containing group MM5 (90–130 nm), which was probably because of the higher molecular weight and bigger volume of GFP. The concentration of DNR in mixed micelles was quantified by dissolve MM1 in DMSO and the UV absorbance of released DNR was recorded. According to the working curve measured using standard DNR solutions, the drug concentration was obtained (7.69%). Concentrations of GFP and Apoptin were obtained in a similar way and the values were 13.90% and 10.86%, respectively.

Zeta potential of the polymer micelles without TAT was measured to be zero due to the neutrality of PEG. The conjugation of TAT, which contains high basic amino acid sequences (i.e., arginine or lysine), dramatically increased the zeta potential to a positive value of 17.98 mV for the TAT-PEG-PLA micelles. On the other hand, the value of the mixed micelles was 1.21 and this was attributed to the low surface density of TAT exposed to the surface. It should be noted that this positive surface charge is beneficial for intracellular drug delivery as it could electrostatically bind to the negatively charged glycosaminoglycans on cellular membranes to enhance the probability of being internalized into the cytoplasm.[25]

Stability of MM1 was conducted by immersion in RPMI 1640 in a concentration of 1 mg/mL.[23] As shown in Figure 7, the particle size did not change significantly even after 96 h of incubation with 10% serum, and no precipitation or aggregation was observed.

Cytotoxicity and *In Vitro* Evaluation of the Mixed Micelles

DNR or daunomycin (daunomycin cerubidine) is a chemotherapeutic agent of the anthracycline family that has been widely used in clinics for the treatment of a broad spectrum of cancers. In our study, due to its intrinsic high fluorescence as well as anticancer efficiency, DNR was firstly selected as a model drug to thoroughly explore the penetrating behavior of the TAT-modified mixed micelles.

The uptake of both MM1 and MM2 into A549 and Caski cell lines could be clearly observed through fluorescence microscope by detecting the red fluorescence from conjugated DNR. The fluorescence in the cells kept increasing even after 36 h culture, indicating a good accumulation and retention capacity of the mixed micelle system (Figure 8). The key mechanism for macromolecules to be entrapped in tumors without immediate clearance was found to be retention, whereas low-molecular-weight substances were not retained but returned to blood circulation by diffusion.[26] Therefore, high-molecular-weight advantage of the mixed micelles, nonimmunogenicity of PEG in the outside shell and covalent conjugation of drug may contribute to the prolonged circulation and accumulation. It is noteworthy that the fluorescence intensity of MM1 groups (TAT-modified) was much stronger than that of MM2 groups (without TAT), implying the enhanced uptake from the TAT-mediated cell membrane penetration.

The translocation efficacy of TAT was quantitatively confirmed by MTT assay. As shown in Figure 9(a), mixed micelles MM1 induced more growth inhibition of Hela cells, compared to control sample MM2 without TAT. The remarkable phenomena happened to Caski cell lines as well, except for the highest concentration, where MM1 and MM2 did not show significant

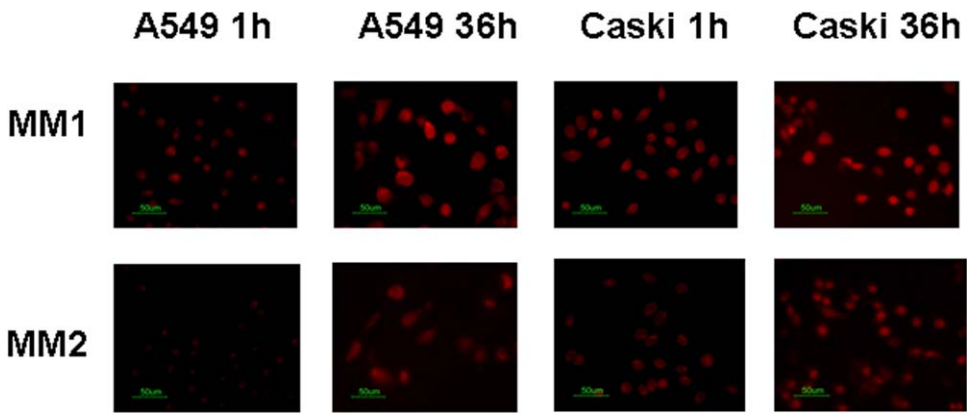

Figure 8. Microscopic images of A549 and Caski cells cultured with MM1 and MM2. [Color figure can be viewed in the online issue, which is available at wileyonlinelibrary.com.]

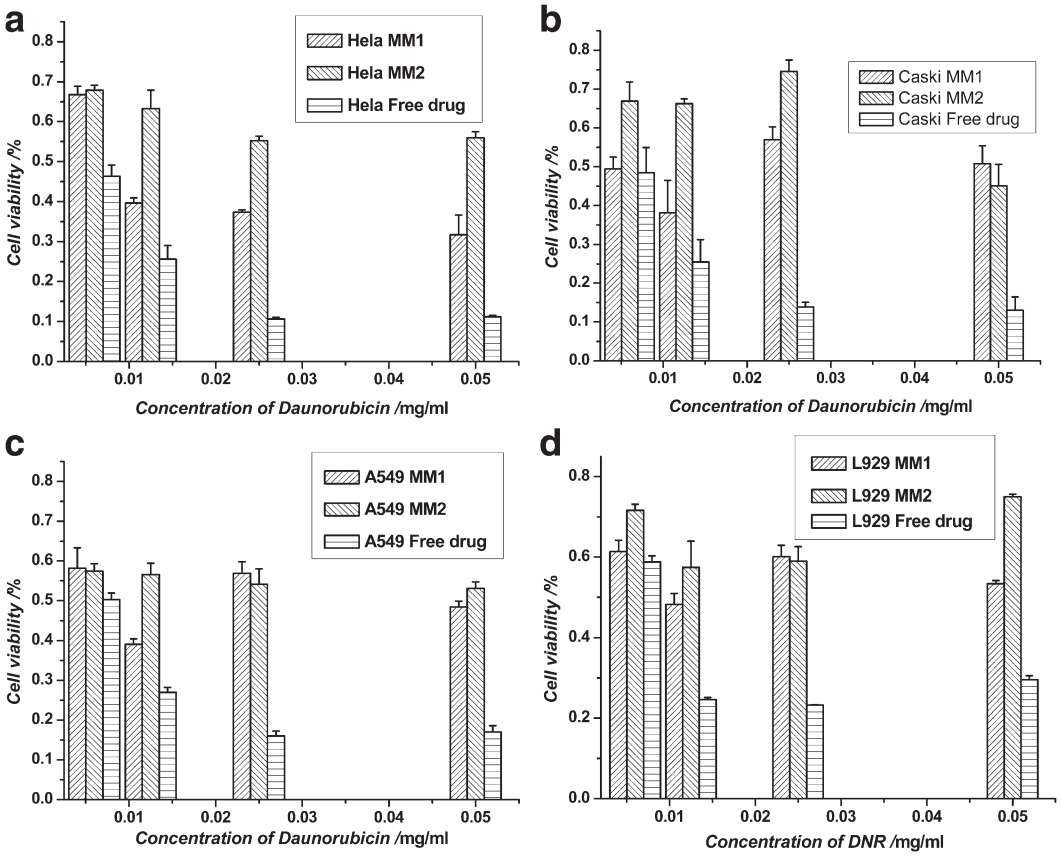

Figure 9. Cytotoxicity studies of MM1 and MM2 against Hela (a), Caski (b), A549 (c), and L929 (d) cell lines at different drug concentrations, evaluated by MTT assay after 24 h culture.

differences probably due to the excess amount of the applied DNR [Figure 9(b)]. In contrast to Hela and Caski, MM1 and MM2 appeared to play the same role in A549 and L929 cell lines without significant difference [Figure 9(c,d)]. From the above data a conclusion can be drawn that TAT containing mixed micelles induced more cell growth inhibition in both Hela and Caski cell lines in comparison with control micelles without TAT. Furthermore, the enhanced translocation of TAT does not always happen to all the tumor cells, but more likely happen to some specific cell lines (in our case, Hela and Caski). This discovery tells us that it is important to evaluate the sensitivity of the tumor cell to TAT to determine the suitable model before designation.

Although TAT showed excellent enhanced drug uptake for DNR-loaded mixed micelles, this conclusion could not be directly applied for Apoptin transportation. Unlike DNR, Apoptin is a hydrophilic protein with much larger molecular weight of 13.6 kDa and bigger particle size. It should be pointed out that the mixed micelles containing proteins (like GFP or Apoptin) were all formed at the IPs (isoelectric point) of proteins to ensure the proteins to be encapsulated into the hydrophobic core of the micelles. Before the further investigation, hydrophilic GFP with similar particle size and water solubility to Apoptin was first encapsulated into the mixed micelles (MM3) as a model of Apoptin-loaded ones. Probably because of the higher molecular weight, the apparently different behavior of TAT-modified GFP-loaded mixed micelles compared to MM4 could not be clearly exhibited. In order to obtain a better visualization of GFP-containing micelles, small amount of DMSO (3%) was adopted just as a tool to enhance the cellular uptake. It has to be mentioned that the DMSO application *in vivo* is still not acceptable, however, according to our previous *in vitro* study,

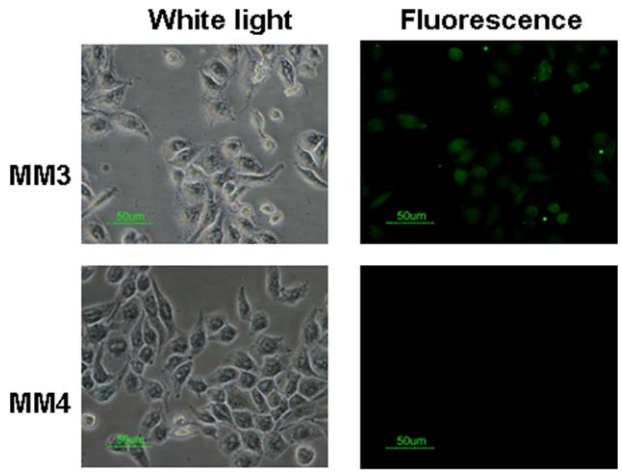

Figure 10. Microscopic images of Caski cells culture with MM3 (up) and MM4 (down) in the presence of 3% DMSO. [Color figure can be viewed in the online issue, which is available at wileyonlinelibrary.com.]

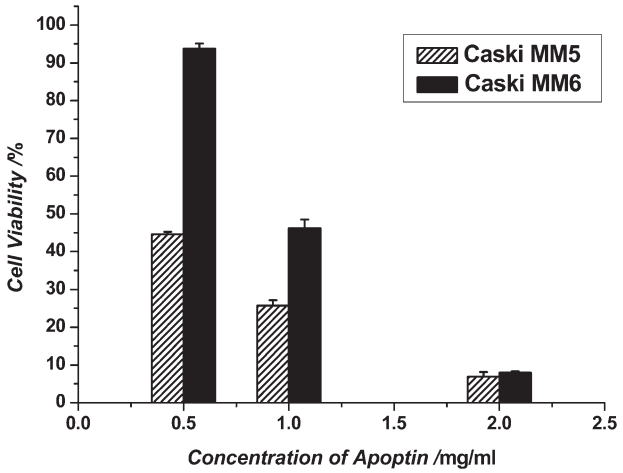

Figure 11. Cytotoxicity study of MM5, MM6 against Caski cell lines at different drug concentrations, evaluated by MTT assay after 24 h culture.

10% of DMSO treatment up to 2 h has very little repressive effect on cell growth and it could be used as penetration enhancer for GFP *in vitro*.[8] In this case, the uptake enhancement ability induced by TAT seemed to be limited but still obvious by comparing the fluorescence difference between MM3 and MM4 cultured Caski cells (Figure 10). The results also implied that the transportation of the hydrophilic protein into cells could be possible. In the case of Apoptin-loaded mixed micelles as our final target product for future *in vivo* application, the DMSO strategy is no longer necessary. The more obvious TAT assistance could be observed without using any DMSO, which is probably due to the molecular and size differences of GFP and Apoptin. Comparing to MM6 without TAT, MTT assay clearly showed that MM5 with TAT modification could kill much more tumor cells even at very low drug concentration, indicating the prominent TAT penetration enhancement and sufficient killing effect of the tumor cells (Figure 11). Apoptin shows different localization in tumor cells and normal cells: it predominantly accumulates in nucleus of tumor cells as a multimeric protein complex and associates in tumor cells with chromatin structures.[27] While in normal cells, it is detected mainly in cytoplasm. There are various implicated mechanisms concerning Apoptin-mediated cell death and it has been recognized that the particular domains control nucleocytoplasmic shuttling of Apoptin, phosphorylation on specific residue and varies relevant signaling contribute to Apoptin's activity, and the partners interacted with Apoptin regulate activity or subcellular localization of Apoptin.[28]

Two major cell entry routes may contribute to the cytosolic translocation of this kind of CPP–cargo complexes: the direct cell membrane penetration and the endosomal pathway. Some CPPs may promote the internalization of the cargo molecule through direct penetration across the plasma membrane; still, the majority of CPPs attached to a cargo molecule utilize the endocytic machinery to gain entry to cells. For example, the caveolae have been demonstrated to mediate the cellular uptake of the fusion protein of Tat peptide with GFP.[29,30] Herein, cellular uptake by Hela cells was examined by CLSM (Figure 12). Combining the blue fluorescence of the nuclei (DAPI) and the red fluorescence of DNR, the merged purple fluorescence in the nuclei indicates that MM1 are mainly located in the nuclei. The punctuated dot-shaped fluorescence in cytoplasm indicated that the delivery system adopted here also gained the cell entry through endocytosis pathway, since its direct penetration facilitated by the conformational change of TAT was probably prohibited due to the preformed micelle structure. Then the DNR molecules were released and diffused through endocytic compartments to the nucleus eventually, similar as the nuclear accumulation of naked drug.[31,32] It has also been reported that endosomal route prevails in the uptake of bigger cargoes such as proteins, liposomes, and nanoparticles.[33]

It was expected that, with the cooperation of TAT and EPR effect, the prepared nanomicelles could enter tumor sites easily and then degrade. Subsequently, Apoptin, which was conjugated to the hydrophobic part of mPEG-*b*-P(LA-*co*-MCC), was exposed to the cytoplasm and located in the nuclear of tumor cell specifically. The excellent inhibition effect on tumor cells should be attributed to the perfect combination of TAT and Apoptin in this kind of mixed micelle system. In addition to the tumor-selective apoptosis characteristics, it is noteworthy that Apoptin is independently associated with p53 and Bcl-xL and even stimulated by Bcl-2 sometimes, which indicates that it can take effect in the cases where chemotherapeutics fail.[34–36]

CONCLUSIONS

In this study, we developed a multifunctional mixed micelle system by coassembling TAT-PEG-PLA and mPEG-*b*-P(LA-*co*-

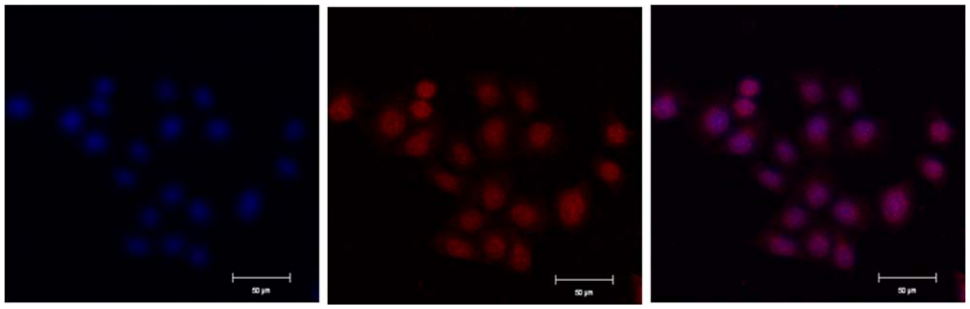

Figure 12. Confocal laser scanning micrographs of Hela cells treated with MM1. From left to right: the DAPI (blue) fluorescence for the nuclei; DNR (Red) fluorescence for MM1; overlay of the two images. Scale bar = 50 μm. [Color figure can be viewed in the online issue, which is available at wileyonlinelibrary.com.]

MCC/DNR(GFP or Apoptin)) as drug delivering system. These copolymer systems were characterized by NMR, DLS, TEM, UV-Vis, MALDI-TOF and XPS. The results of MTT revealed that mixed micelles containing both TAT and DNR, exhibited better cell penetrating capacity and tumor cytotoxicity to Hela and Caski cell lines in comparison with the control micelles without TAT. Sensitivity of the tumor cells to TAT appeared to be an important factor for the evaluation of the enhanced membrane penetration by TAT. The huge hydrophilic protein (like GFP) containing mixed micelles could also be transferred into cells with the enhancement of DMSO. Finally, the TAT-modified Apoptin-loaded mixed micelles could successfully enter the tumor cells and induced large amount of cell growth inhibition. The encouraging results revealed the great potential of the multifunctional mixed micelles to be applied as anti-cancer drug delivery and tumor specific apoptosis.

ACKNOWLEDGMENTS

The authors would like to thank the financial support from the National Natural Science Foundation of China (No. 21174143, 51021003, and 20774094), the Ministry of Science and Technology of China (No. 2009CB930102; 863 Project, No. SS2012AA020603), "100 Talents Program" of the Chinese Academy of Sciences (No.KGCX2-YW-802), and Jilin Provincial Science and Technology Department (No. 20100588).

REFERENCES

1. Szebeni, J.; Muggia, F. M.; Alving, C. R. *J. Natl. Cancer Inst.* **1998**, *90*, 300.
2. Saif, M. W.; Kim, R. *Expet. Opin. Pharmaco.* **2007**, *8*, 2719.
3. Nakazato, K.; Kim, C.; Terajima, K.; Murata, S.; Fujitani, H.; Nakanishi, K.; Tajima, H.; Kumazaki, T.; Sakamoto, A. *J. Cancer Res. Clin. Oncol.* **2007**, *133*, 741.
4. Seow, W. Y.; Xue, J. M.; Yang, Y. Y. *Biomaterials* **2007**, *28*, 1730.
5. Zhan, C. Y.; Gu, B.; Xie, C.; Li, J.; Liu, Y.; Lu, W. Y. *J. Controlled Release* **2010**, *143*, 136.
6. Xie, Z. G.; Hu, X. L.; Chen, X. S.; Lu, T. C.; Liu, S.; Jing, X. B. *J. Appl. Polym. Sci.* **2008**, *110*, 2961.
7. Musacchio, T.; Laquintana, V.; Latrofa, A.; Trapani, G.; Torchilin, V. P. *Mol. Pharm.* **2009**, *6*, 468.
8. Wang, H.; Zhong, C. Y.; Wu, J. F.; Huang, Y. B.; Liu, C. B. *J. Controlled Release* **2010**, *143*, 64.
9. Lindgren, M.; Rosenthal-Aizman, K.; Saar, K.; Eiriksdottir, E.; Jiang, Y.; Sassian, M.; Ostlund, P.; Hällbrink, M.; Langel, U. *Biochem. Pharmacol.* **2006**, *71*, 416.
10. Nori, A.; Jensen, K. D.; Tijerina, M.; Kopeckova, P.; Kopecek, J. *J. Controlled Release* **2003**, *91*, 53.
11. Paschke, M.; Hohne, W. *Gene* **2005**, *350*, 79.
12. Nitin, N.; LaConte, L. E.; Zurkiya, O.; Hu, X.; Bao, G. *J. Biol. Inorg. Chem.* **2004**, *9*, 706.
13. Chikh, G.; Bally, M.; Schutze-Redelmeier, M. P. *J. Immunol. Methods* **2001**, *254*, 119.
14. Cheng, C. M.; Huang, S. P.; Chang, Y. F.; Chung, W. Y.; You, C. Y. *Biochem. Biophys. Res. Commun.* **2003**, *305*, 359.
15. Danen-Van Oorschot, A. A.; Fischer, D. F.; Grimbergen, J. M.; Klein, B.; Zhuang, S.; Falkenburg, J. H.; Backendorf, C.; Quax, P. H.; Van der Eb, A. J.; Noteborn, M. H. *Proc. Natl. Acad. Sci. USA* **1997**, *94*, 5843.
16. Sawant, R. R.; Torchilin, V. P. *Int. J. Pharm.* **2009**, *374*, 114.
17. Lee, E. S.; Gao, Z.; Kim, D.; Park, K.; Kwon, I. C.; Bae, Y. H. *J. Controlled Release* **2008**, *129*, 228.
18. Guan, H. L.; Xie, Z. G.; Tang, Z. H.; Xu, X. Y.; Chen, X. S.; Jing, X. B. *Polymer* **2005**, *46*, 2817.
19. Yue, J.; Li, X. Y.; Mo, G. J.; Wang, R.; Huang, Y. B.; Jing, X. B. *Macromolecules* **2010**, *43*, 9645.
20. Yue, J.; Wang, R.; Liu, S.; Wu, S. H.; Xie, Z. G.; Huang, Y. B.; Jing, X. B. *Soft Matter* **2012**, *8*, 3426.
21. Demeneix, B.; Hassani, Z.; Behr, J. P. *Curr. Gene Ther.* **2004**, *4*, 445.
22. Hu, X. L.; Liu, S.; Huang, Y. B.; Chen, X. S.; Jing, X. B. *Biomacromolecules* **2010**, *11*, 2094.
23. Ebrahim Attia, A. B.; Yang, C.; Tan, J. P. K.; Gao, S. J.; Williams, D. F.; Hedrick, J. L.; Yang, Y. Y. *Biomaterials* **2013**, *34*, 3132.
24. Xiong, X. B.; Uludag, H.; Lavasanifar, A. *Biomaterials* **2010**, *31*, 5886.
25. Console, S.; Marty, C.; Garcia-Echeverria, C.; Schwendener, R.; Ballmer-Hofer, K. *Biol. Chem.* **2003**, *278*, 35109.
26. Maeda, H.; Wu, J.; Sawa, T.; Matsumura, Y.; Hori, K. *J. Controlled Release* **2000**, *65*, 271.
27. Grimm, S.; Noteborn, M. *Trends Mol. Med.* **2010**, *16*, 88.
28. Zhou, S. N.; Zhang, M. X.; Zhang, J.; Shen, H.; Tangsakar, E.; Wang, J. S. *Med. Oncol.* **2012**, *29*, 2985.
29. Ferrari, A.; Pellegrini, V.; Arcangeli, C.; Fittipaldi, A.; Giacca, M.; Beltram, F. *Mol. Ther.* **2003**, *8*, 284.
30. Fittipaldi, A.; Ferrari, A.; Zoppe, M.; Arcangeli, C.; Pellegrini, V.; Beltram, F.; Giacca, M. *J. Biol. Chem.* **2003**, *278*, 34141.
31. Shuai, X.; Ai, H.; Nasongkla, N.; Kim, S.; Gao, J. *J. Controlled Release* **2004**, *98*, 415.
32. Kuang, H. H.; Wu, S. H.; Xie, Z. G.; Meng, F. B.; Jing, X. B.; Huang, Y. B. *Biomacromolecules* **2012**, *13*, 3004.
33. Räägel, H.; Säälik, P.; Pooga, M. *Biochim. Biophys. Acta* **2010**, *1798*, 2240.
34. Zhuang, S. M.; Shvarts, A.; vanOrmondt, H.; Jochemsen, A. G.; van der Eb, A. J.; Noteborn, M. H. *Cancer Res.* **1995**, *55*, 486.
35. Schoop, R. A.; Kooistra, K.; Baatenburg De Jong, R. J.; Noteborn, M. H. *Int. J. Cancer* **2004**, *109*, 38.
36. Liu, X.; Elojeimy, S.; El-Zawahry, A. M.; Holman, D. H.; Bielawska, A.; Bielawski, J.; Rubinchik, S.; Guo, G. W.; Dong, J. Y.; Keane, T.; Hannun, Y. A.; Tavassoli, M.; Norris, J. S. *Mol. Ther.* **2006**, *14*, 637.